TUNABLE IMMUNOSTIMULATORY NANOCARRIER
FOR IMPROVING CANCER IMMUNOCHEMOTHERAPY

by

Zhuoya Wan

BS, Pharmacy, West China School of Pharmacy, Sichuan University 2015

Submitted to the Graduate Faculty of
School of Pharmacy in partial fulfillment
of the requirements for the degree of
Master of Science

University of Pittsburgh
2017

UNIVERSITY OF PITTSBURGH
SCHOOL OF PHARMACY

This thesis was presented

by

Zhuoya Wan

It was defended on

August, 2017

and approved by

Song Li, Professor, Pharmaceutical Science

Jiang Li, Research Associate Professor, Pharmaceutical Science

Da Yang, Assistant Professor, Pharmaceutical Science

[Thesis Director/Dissertation Advisor]: **Song Li**, Professor, Pharmaceutical Science

TUNABLE IMMUNOMODUALTING 1-D-MT BASED NANOCARRIER

FOR IMPROVING CANCER IMMUNOCHEMOTHERAPY

Zhuoya Wan, BS

University of Pittsburgh, 2017

Chemotherapy is the mainstream method of cancer therapy. In addition to direct cytotoxic effects on tumor cells, chemotherapy can induce antitumor immunity. The shortcomings of traditional chemotherapy are attributed to low solubility in aqueous solutions, rapid elimination, and lack of selectivity. In addition, cancers rapidly establish an immunological tolerance to the chemotherapy-induced antitumor immunity. The immune tolerance and suppression represent a major barrier to successful cancer treatment and are potential target for new therapeutics. Recent evidence demonstrates that an important mechanism underlying the immunological tolerance is the upregulated indoleamine-2,3-dioxygenase (IDO) expression in tumor cells or tumor-associated immune cells. Therefore, IDO pathway inhibition offers a potential for enhanced anti-tumor responses of chemotherapeutic agents.

In our previous study, systemic delivery of paclitaxel (PTX) using the PEG_{2k}-Fmoc-NLG nanocarrier, a PEG-modified prodrug of NLG919 (an IDO1 selective inhibitor), led to a significantly enhanced anti-tumor effect of PTX by reactivating immunogenic responses. In this study we examined the therapeutic potential of a new nanocarrier that is based on a prodrug of 1-methyl-d-trptophan (1-D-MT). 1-D-MT is also an IDO inhibitor but has been reported to enhance antitumor immunity via different mechanism. The nanocarrier will be developed via reversible addition fragmentation transfer

(RAFT) polymerization. In addition to the simplicity of the synthesis of the nanocarrier, the amount of 1-D-MT that can be incorporated into the polymer can be readily tuned via controlling the degree of polymerization.

Two 1-D-MT-based monomers were first synthesized followed by RAFT polymerization to give well-defined di-block co-polymers. Several polymers were synthesized and they varied in the molar ratio of hydrophilic POEG block/hydrophobic 1-D-MT block and the type of linker. Preliminary data showed that a 1-D-MT polymer with ethylene glycol vinyl ether linker can only load limited amounts of PTX and doxorubicin (DOX). Introduction of a vinylbenzyl chloride linker led to an improvement in drug loading capacity. More studies on the biophysical and biological properties of the new carrier are currently underway.

TABLE OF CONTENTS

LIST OF TABLES

LIST OF FIGURES

INTRODUCTION

1.1 CURRENT TREATMENT REGIMEN FOR BREAST CANCER

Chemotherapy can be used as adjuvant and neoadjuvant chemo before or after breast cancer surgery, the benefit of which is particularly pronounced in triple negative (ER-, PR-, HER2-) tumors[1]. The most frequently used therapeutic regimen includes paclitaxel (PTX) and docetaxel and doxorubicin (DOX).
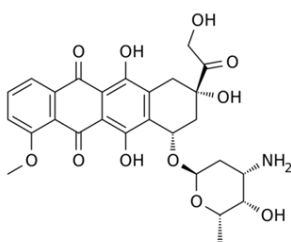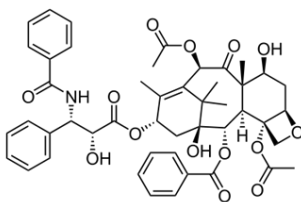
Doxorubicin   **Paclitaxel**   **Docetaxel**
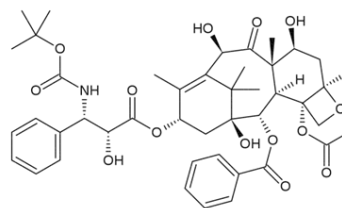
1.2 LIMITATIONS OF TRADITIONAL CHEMOTHERAPY

The general shortcomings of traditional chemotherapy are attributed to **<u>aqueous solubility</u>** and **<u>lack of selectivity</u>**.

1.2.1 Aqueous Solubility

The poor water-solubility of the aforementioned compounds is due to their bulky polycyclic structure, based on which it is hard for those high lattice energy molecules to dissolve in aqueous solutions. In addition, the bulky polycyclic nature makes it difficult for those molecules to form hydrogen bonds with water[2]. The solubility issue of anticancer drugs is further magnified when taking intravenous administration into consideration[3] because most anticancer drugs are delivered

intravenously in clinical application. As for those irritating anticancer drugs, intravenous infusion is usually applied to achieve a more desirable pharmacokinetic profile and prevent gastrointestinal toxicity. A drug with poor solubility is unviable for this route of administration. Thus, these drugs deserve more attention in order to make them safe and effective for clinical applications.

1.2.2 Lack of Selectivity

The other major problems of anticancer drugs are associated with the effect of their toxicities on healthy cells and the difficulty for them to be delivered efficiently to designated sites.

The mechanisms of action (MOA) of those compounds are largely focused on inhibition of DNA synthesis and cell division[4]. Therefore, they are highly efficient at killing cancer cells that are dividing at a much faster rate than most of normal cells[5]. However, some healthy cells also have high proliferation rates, such as the cells in the hair follicles[6], digestive tract and bone marrow[5]. As for those cells, they are also sensitive to anticancer drugs. This results in severe side-effects, including hair loss, inflammation of the lining of the digestive tract, and decreased production of blood cells and immune cells.

In addition, anticancer drugs are broadly distributed in all body tissues after the intravenous injection, which significantly limits the efficiency of their delivery to tumor tissues[5]. It has been reported that less than 5% of those anticancer drugs can reach the tumor sites. Therefore, large doses of anticancer drugs are given to patients aiming to achieve effective dosage at designated sites. However, this strategy results in undesirable side effects at the same time because it can increase the distribution of anticancer drugs in normal tissues. Thus, there is an urgent need to improve the distribution profiles of anticancer drugs.

Table 1. Solubility, Partition Coefficient Data and Mechanisms of Selected Anticancer Drugs

Drug	Aqueous Solubility (25°C)*f	Partition Coefficient	Category	Function
Chemotherapeutic drugs				
Paclitaxel	<0.3 ug/mL	3.5	Mitosis inhibitors	Target microtubules and associated proteins required in cell division
Docetaxel	4.93 ug/mL	2.92		
Doxorubicin. HCl	2.6 mg/ml	0.52	Antitumor antibiotics	Bind DNA to prevent DNA and/or RNA synthesis

Biopharmaceutics Classification System (BCS): poorly water-soluble drug was defined as the drug that its highest dose strength is not or less soluble in 250ml of aqueous media over the PH range of 1 to 7.5.

1.3 PROSPECTIVE OF NANOMEDICINE IN CANCER THERAPY

Nanotechnology has its distinctive features for drug delivery by enhancing the pharmaceutical properties of therapeutic agents[7]. These vehicles can improve the solubility of water-insoluble drugs and meanwhile increase efficacy or reduce toxicities of therapeutic molecules by improving their distribution at desired target sites. Those features encourage people to apply this technology to cancer therapy. Until now, there are a number of nanocarrier systems under investigation around the world. Among all the platforms, liposomes, albumin nanoparticles and polymeric micelles have been approved for cancer treatment[8]. Many other nanotechnologies have demonstrated great potentials in preclinical studies and are currently under clinical investigation.

1.3.1 EPR Effect for Passive Targeting

The preferential accumulation of intact nanoparticles within solid tumors is generally attributed to the leaky tumor vessels and poor lymphatic drainage systems of the tumor tissues, known as the

enhanced permeability retention (EPR)[9] effect. The enhanced permeability of the leaky tumor vasculatures facilitates the entry of nanoparticles into the tumor interstitial space given that the sizes of the particles are in the range of 100~500 nm. On the other hand, the poorly developed lymphatic drainage systems increase the retention times of those nanoparticles within solid tumor tissues. The aforementioned effect is fundamental for the selectivity and therapeutic activity of those nanoparticles, which was well characterized in xenografted human and murine models in mice. Recently, the existence of this phenomenon in human tumors has been published by Lee and Davis group. The Mark E. Davis group[10] observed that CRLX101 nanoparticles, consisting of a cyclodxtrin-based polymer and camptothecin, can accumulate in gastric tumors following intravenous injection in a clinical trial of five patients. In addition, the accumulation of ^{64}Cu-labled nanoparticles[11] within tumor sites was found in patients, the results of which were validated by PET/CT imaging. The aforementioned evidence of ^{64}Cu-labled nanoparticles establishes that the EPR effect is present in human metastatic tumors.

1.3.2 Polymeric Micelles as Nanocarriers for Cancer Treatment

Polymeric micelles are an aggregate of block amphiphilic copolymers (di-block, tri-block and graft block), homogenously dispersed in aqueous solutions. They are regarded as one of the most promising modalities among all drug carriers. Usually, polymeric micelles have a core-shell structure, composed of an inner hydrophobic core and an outer hydrophilic shell. The hydrophobic core can provide a loading space for poorly water-soluble drugs due to hydrophobic-hydrophobic interactions. The surrounded hydrophilic shell helps to improve the solubility of those limited-solubility drugs. The most commonly used hydrophilic segment was polyethylene glycol (PEG), which is a safe, non-toxic and biodegradable polymer. Apart from enhancing their solubility, PEG modification enhances the stability of polymeric

4

micelles and increases their circulation time in the blood. At first, PEG reduces the undesirable aggregation of polymeric micelles through secondary interactions among those particles. In addition, PEG modifications prevent the recognition and binding of plasma proteins, minimizing the nonspecific uptake of polymeric micelles by the reticuloendothelial system (RES).

The growing interest of polymeric micelles is attributed to their attractive features. Polymeric micelles can be prepared by an easy method and can be sterilized simply by filtration, taking advantage of their small sizes (10nm-100nm). Compared with micelles formed by low-molecule surfactants, these micelles are more kinetically stable. In addition, polymeric micelles can preferentially accumulate at tumor sites through the EPR effect. One prominent advantage of polymeric micelles is that they can be easily modified to achieve functional and tunable effects. Currently, several polymeric micelles are under clinical investigation[8] such as Genexol-PM, NK-105 and CRLX-001, among which Genexol-PM was approved in South Korea for breast cancer and non-small-cell lung carcinoma (NSCLC) treatment.

1.3.3 Rationale of Combination Therapy Using Pharmacologically Active Polymeric Micelles

The stability of polymeric micelles largely depends on the type and molecular weight of their hydrophobic block[12]. In most cases, the higher the molecular weight of a hydrophobic domain, the more stable the polymeric micelles are. Nonetheless, most of the carrier materials do not have biological activities other than the function of delivery. The use of large amounts of carrier materials also raises some safety concerns[13]. One strategy to address this issue is to use hydrophobic therapeutic agents to replace the inert internal domains of the polymeric micelles. These prodrugs-based carriers not only solve the solubility issue of internal hydrophobic drugs by conjugating them with a hydrophilic

polymeric shell, but also prevent the burst release of the aforementioned internal domain through modulating their release profile.

In addition, monotherapy based on an individual drug has some limitations such as drug resistance, narrow therapeutic windows and inevitable side effects induced by high dosages of a single drug. Therefore, this type of pharmacologically active vehicle provides a unique strategy to achieve combination therapy, which circumvents the aforementioned problems through the loading of another poorly water-soluble drug within the hydrophobic core. By applying such a pharmacologically active carrier, the overall antitumor effects can be enhanced by a synergistic effect achieved through simultaneous co-delivery of two drugs to tumor sites.

1.4 1-D-MT BASED NANOCARRIER SYSTEMS

1.4.1 Combination of Chemotherapy and Immunotherapy

The combination of traditional chemotherapeutic agents and immunotherapies is regarded as a valid therapeutic approach to cancer treatment[14], which was supported by data from clinical studies. The mechanism behind this successful combination might due to the enhanced immune response of conventional anticancer drugs in addition to their direct killing effects on tumor cells. Taxanes (paclitaxel and docetaxel) and anthracycline (doxorubicin) are the most popular chemotherapeutics in clinical application for breast cancer treatment. Those drugs can induce a protective immune response[15], which might help to enhance the overall antitumor efficacy[16]. However, the effectiveness of those chemotherapeutics-induced immune responses is limited by a variety of feedback suppressive circuits during tumor development and cancer treatment.

Therefore, a blockade of inducible negative feedback mechanisms represents one of the most promising approaches to enhance the immune response for cancer treatment. Indeed, exciting results have been obtained from preclinical and clinical trials with the use of the CTLA-4 and PD-1 pathway inhibitors, known as Ipilimumab (Yevoy®) and Nivolumab (Opdivo®)[17]. The aforementioned CTLA-4 and PD-1 are two important inhibitory proteins involved in immune checkpoint pathways and their expressions are upregulated on activated T cells. Indoleamine 2,3-dioxygenase (IDO) is another counter regulatory protein, which plays an important role in generating an immunosuppressive microenvironment. Interestingly, IDO enzyme is reported to interact both with CTLA-4 and PD-1 checkpoints via complex loops that are not clearly elucidated[18,19]. Based on the existing evidence, the expression of CTLA-4 on regulatory T (Treg) cells leads to upregulation of IDO enzymes on dendritic cells (DCs), while the upregulated IDO enzymes can increase the expression of PD-1 on Treg cells.

1.4.2 IDO is a Potential Therapeutic Target for Enhancing Immune Response

L-Tryptophan is known as an essential amino acid with a typical indole ring on its structure, which can be metabolized to kynurenine by three distinctive IDO enzymes[20], including indoleamine 2,3-dioxygenase 1 (IDO1), indoleamine 2,3-dioxygenase 2 (IDO2), and tryptophan 2,3-dioxygenase (TDO). Generally, the IDO enzyme was found to be upregulated in the tumor cells themselves, in tumor associated endothelial cells as well as in some host immune cells such as macrophages and dendritic cells during the late stage of tumorigenesis, which directly or indirectly participates in the immunosuppressive pathway.

The decreased amount of tryptophan activates the stress-response kinase GCN2, which leads to inhibition of the proliferation of T cells (CD4$^+$ T cells and CD8$^+$ T cells), and a biased differentiation of

naïve CD4^{+} T cells toward Treg cells. The increased kynurenine metabolites are capable of activating the aryl hydrocarbon receptor (AhR), which causes a biased differentiation of macrophages toward tumor associated macrophages (TAMs), an immunosuppressive phenotype. In addition, the IDO enzymes and IDO-activated Treg cells are highly associated with the increased suppressive function of myeloid-derived suppressor cells (MDSC). The increased infiltration of MDSCs, Tregs and TAMs is an important clinical indicator for poor patient prognosis and possible resistance to therapies. Therefore, the pharmacological inhibition of IDO enzymatic activity represents a promising approach to enhance immune response. For these reasons, numerous IDO inhibitors have been developed for increasing the therapeutic efficacy of cancer treatment. [19]

Table 2. IDO pathway inhibitors in clinical trials

IDO Pathway Inhibitors	Clinical Trials
Indoximod	**Phase II (multiple)**
Epacadostat (INCB024360)	Phase II (multiple)
GDC-0919 (NLG919)	Phase I/II (multiple)
BMS-986205	Phase I (Entry)
PF-06840003	Phase I (Entry)

1.4.3 1-Methyl-Trptophan

1.4.3.1 1-Methyl-D-Tryptophan (Indoximod)

1-methyl-D, L-tryptophan (1-D, L-MT), a racemic mixture of two stereoisomers (1-D-MT, 1-L-MT), is one of the first well-studied IDO inhibitors. There has been a long-standing debate as to which stereoisomer is superior for cancer immunotherapy. Interestingly, the L counterpart of 1-MT has a higher potency in cell based assays, while its D counterpart has proved to be more effective regarding

immunostimulatory effects in *vivo*[21]. Hence, 1-methy-D-tryptophan (indoximod) is selected as the potential candidate in clinical trials as an adjunct approach to conventional chemotherapy.

Table 3. Ongoing clinical trials testing the clinical profile of indoximod in cancer patients [21]

Indications	Phase	Status	Notes	Reference
Brain neoplasms	I/II	Recruiting	Combined with temozolomide	NCT02052648
Breast carcinoma	I/II	Active, not recruiting	Combined with an experimental DC-based vaccine	NCT01042535
	II	Recruiting		NCT01792050
			Combined with docetaxel	
Melanoma	I/II	Recruiting	Combined with ipilimumab	NCT02073123
Pancreatic carcinoma	I/II	Not yet Recruiting	Combined with gemcitabine and paclitaxel	NCT02077881
Prostate carcinoma	II	Recruiting	Combined with sipuleucel-T	NCT01560923

1.4.3.2 Unclear Mechanism of Action by 1-Methyl-D-Tryptophan

1-D-MT was firstly known as an IDO1-specific inhibitor. One remaining puzzling issue has been the fact that this compound does not exhibit a significant inhibitory activity on IDO1 enzyme *in vitro*, but somehow shows an effect that closely mimics the biological consequence of IDO1 enzymatic inhibition *in vivo.*

Experimental evidence accumulated from a large number of studies has confirmed that 1-D-MT does participate in the inhibition of IDO1 pathway. However, the current experimental data also point to the conclusion that 1-D-MT might be involved in several other mechanisms: 1) preferential inhibition of the IDO2 isoform[22]; 2) racemization of the D-isomer to the L-counterpart or alternative formation of 1-D-MT metabolites *in vivo*; 3) inhibition of tryptophan transport; 4) inhibition of WARS1 or WARS2, the enzymes which are involved in tryptophan sensing; 5) alteration of autophagy or bypassing the mTOR-inactivated mechanisms under the conditions of amino acid deprivation. These mechanisms warrant further investigation.

1.4.3.3 Pharmacokinetics and Formulations of 1-Methyl-D-Tryptophan

Indoximod is an oral medication with a favorable pharmacokinetic (PK) profile ($T_{1/2}$~10h, Tmax~3h) and a good safety profile in animals[23]. However, clinical pharmacokinetic studies have demonstrated that indoximod failed to exhibit linear PK characteristics at doses above 800mg/kg and up to 2000mg/kg, with its maximum drug exposure levels ($AUC_{(0\sim last)}$) of ~100uM.h and plasma concentration (Cmax) of 15uM. This is different from studies in mice in which greater drug exposure (>300uM.h) and higher Cmax (>20uM) can be achieved via oral dosing at 200 mg/kg b.i.d.[24] Thus, the therapeutic activity of this investigational drug might be limited and it is desirable to increase the drug exposure and Cmax so as to reach better levels for therapeutic efficacy. However, this problem cannot be solved merely by increasing the doses of this drug to patients due to its non-linear PK profile.

For these reasons, different formulation forms of indoximod have been investigated such as salts, spray dry dispersion and a series of prodrugs with different salt forms. Nevertheless, the results of these studies showed that only a few selected prodrugs can result in improved solubility and increased *in vivo* exposure upon oral administration[24]. In addition, there are other issues that negatively affect the therapeutic efficacy such as fast blood clearance of small molecules, which necessiates frequent dosing regimens. These existing have prompted us to develop an intravenous strategy for improving the bioavailability of indoximod at tumor tissues.

1.4.4 PEG-Derivatized 1-D-MT Based Dual Functional Nanocarrier Systems

The free base form of 1-D-MT is barely soluble in aqueous solutions. One common strategy to enhance the solubility of hydrophobic drugs is to solubilize them in organic solvents at first and then dilute this stock solution with aqueous buffers[2]. However, the solubility of 1-D-MT in these organic

solvents is limited as well, such as tetrahydrofuran (THF), dimethyl sulfoxide (DMSO), and methanol and dimethylformamide (DMF). It is difficult to load 1-D-MT into a micelle carrier due to the limited solubility of 1-D-MT in both volatile solvents and aqueous solvents. In order to address this issue, 1-D-MT can be conjugated with PEG to generate a "PEGylated polymeric prodrug" to enhance its solubility in aqueous solutions. An additional advantage is that the PEG modification can prevent the rapid elimination of these small molecules and prolong their circulation time in the body due to the following reasons: 1) PEG has shielding effects by masking the 1-D-MT agent from recognition by host immune system (reduced antigenicity and immunogenicity), 2) with the modification of PEG, the overall hydrodynamic size of the 1-D-MT-PEG micelles is increased, which helps to reduce their renal clearance, 3) PEG modification can prevent the interaction of amine group with plasma proteins through the PEG outer shell. Unlike linear PEG, poly(oligo(ethylene glycol) methacrylate) (POEG) is a hydrophilic block chain, which can be polymerized into polymeric backbone in a tunable manner. POEG shall provide similar effects compared to PEG[25].

As previously mentioned, the major application of 1-D-MT in cancer treatment is in combination with another traditional chemotherapeutic agent[21]. We hypothesize that our polymeric micellar carrier that is based on a prodrug of 1-D-MT can simultaneously deliver the 1-D-MT agent and another conventional therapy such as doxorubicin into the tumor sites to achieve a synergistic effect. We have recently shown that delivery of paclitaxel (PTX) using the PEG_{2k}-Fmoc-NLG nanocarrier, a PEG-derivatized prodrug of NLG919, leads to significantly improved tumor immune microenvironment and enhanced antitumor response. NLG919 is also an IDO1 inhibitor but with much higher specificity. In this study we examined the therapeutic potential of a new nanocarrier that is based on a prodrug of 1-methyl-d-trptophan (1-D-MT). 1-D-MT is also an IDO inhibitor but has been reported to enhance antitumor immunity via different mechanism. The nanocarrier will be developed via reversible addition

fragmentation transfer (RAFT) polymerization. In addition to the simplicity of the synthesis of the nanocarrier, the amount of 1-D-MT that can be incorporated into the polymer can be readily tuned via controlling the degree of polymerization.
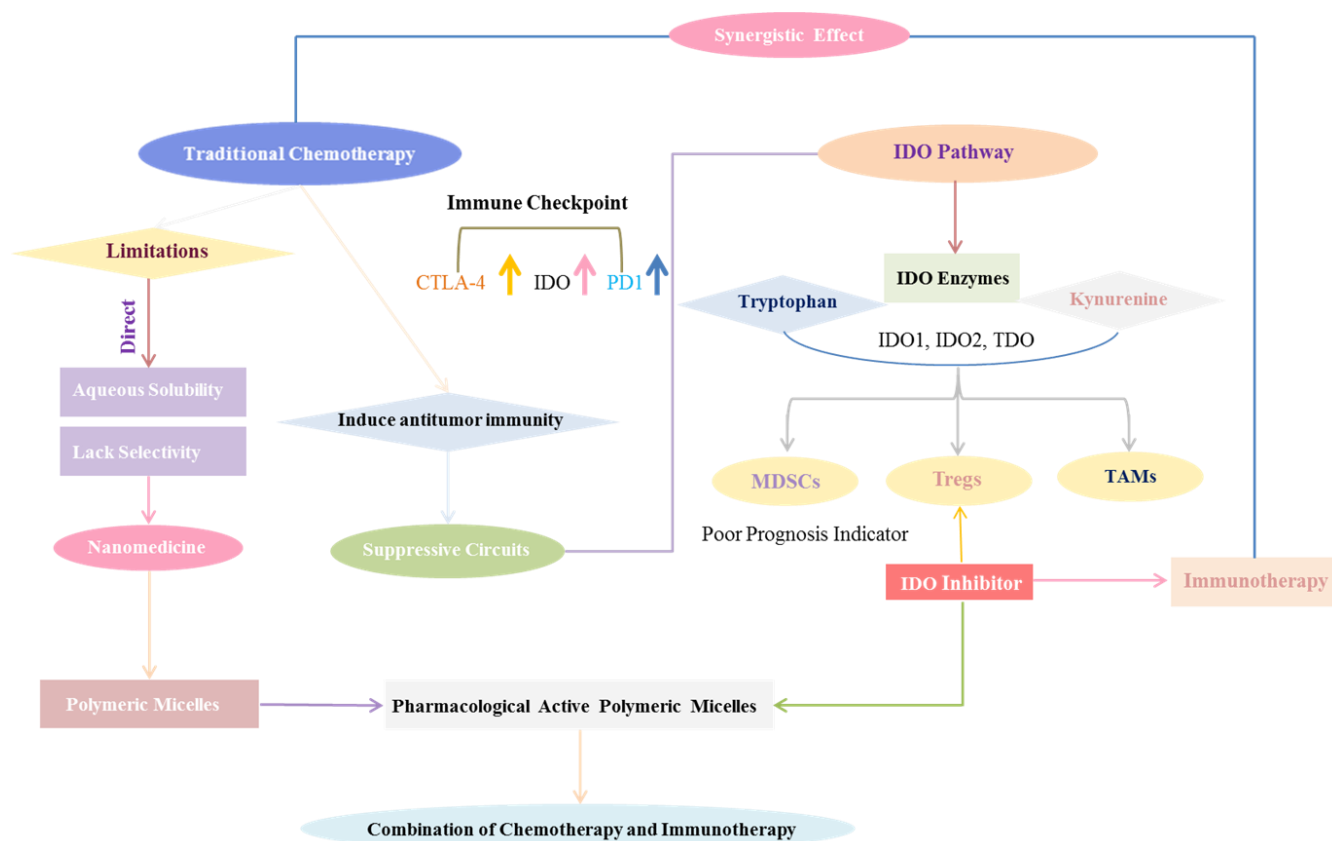
1.5 OVERVIEW OF THE THESIS

Figure 1. Overview of the Design Concept

Two 1-D-MT-based monomers were first synthesized followed by RAFT polymerization[26] to give well-defined di-block co-polymers with five steps. Several polymers were synthesized and they varied in the molar ratio of hydrophilic POEG block/hydrophobic 1-D-MT block and the type of linker. Preliminary data showed that a 1-D-MT polymer with ethylene glycol vinyl ether linker can only load limited amounts of PTX and doxorubicin (DOX). Introduction of a vinylbenzyl chloride linker led to an improvement in drug loading capacity. Interestingly, with the assistance of its primary amine group, it showed potential to interact with plasmid DNA. More studies on the biophysical and biological properties of the new carrier are currently underway.

MATERIALS AND METHODS

2.1 MATERIALS

1-methyl-d-trptophan (1-D-MT) was purchased from Sigma-Aldrich (MO, USA). Vinylbenzyl chloride, potassium carbonate (K_2CO_3), Azobisisobutyronitrile (AIBN), Sodium hydroxide (NaOH), 2-Hydroxyethyl methacrylate, N,N'-Dicyclohexylcarbodiimide (DCC), 4-Dimethylaminopyridine (DMAP) di-tert-butyl dicarbonate, 1,4-Dioxane, Dimethylformamide (DMF), Dimethyl sulfoxide (DMSO), Tetrahydrofuran (THF), Ethylacetate (EA), Doxorubicin hydrochloride (DOX·HCl) was obtained from LC Laboratories (MA, USA), Triethylamine (TEA) ---Fisher Scientific, 4-Cyano-4-[(dodecylsulfanylthiocarbonyl)sulfanyl]pentanoic acid, Poly(ethylene glycol) methyl ether methacrylate (OEGMA, Mn=500);

2.2 SYNTHESIS OF 1-D-MT BASED POLYMERS

2.2.1 Synthesis of Boc-Protected 1-D-MT

1-D-MT (200mg, 0.909mmol, 1.0 eq), NaOH (86mg, 2.15mmol, 2.36 eq) and di-tert-butyl dicarbonate (470mg, 2.15mmol, 2.36eq) were dissolved in a mixed solvent of THF (9ml) and H_2O (9.8ml). [27]The mixture was stirred at room temperature for 48h. THF was evaporated under reduced pressure, and the remaining aqueous layer was acidified with 1N HCl to PH=3. 1-D-MT-Boc was extracted by ethylacetate for three times, and the organic layer was collected and concentrated to give the product as a yellow solid (264mg, 0.825mmol, 90% yield).

2.2.2 Sythesis of POEG MacroCTA

POEG MacroCTA was synthesized and purified following a published literature. Briefly, OEGMA 500 (3.05g, 6.10mmol, 20.5 eq), 4-Cyano-4-[(dodecylsulfanylthiocarbonyl)sulfanyl]pentanoic acid (120mg, 0.297 mmol, 1.0 eq), AIBN (8mg, 0.048mmol) and 5ml anhydrous THF were mixed in a schlenk tube. The mixture was then purged with nitrogen so as to remove the oxygen dissolved in the reaction solvents by using a freeze-pump-thawing method. Then, the tube was immersed in an oil bath at 85°C for 2.5h under nitrogen protection. After polymerization, the reaction was first quenched in a liquid nitrogen bath. Next, the POEG MacroCTA was purified by precipitation and extraction using cold diethyl ether for three times. Finally, POEG was obtained in the form of yellow liquid oil (2.3977g, 91% yield), followed by vacuum drying. The conversion rate was 86% as determined by ^{1}H NMR spectroscopy.

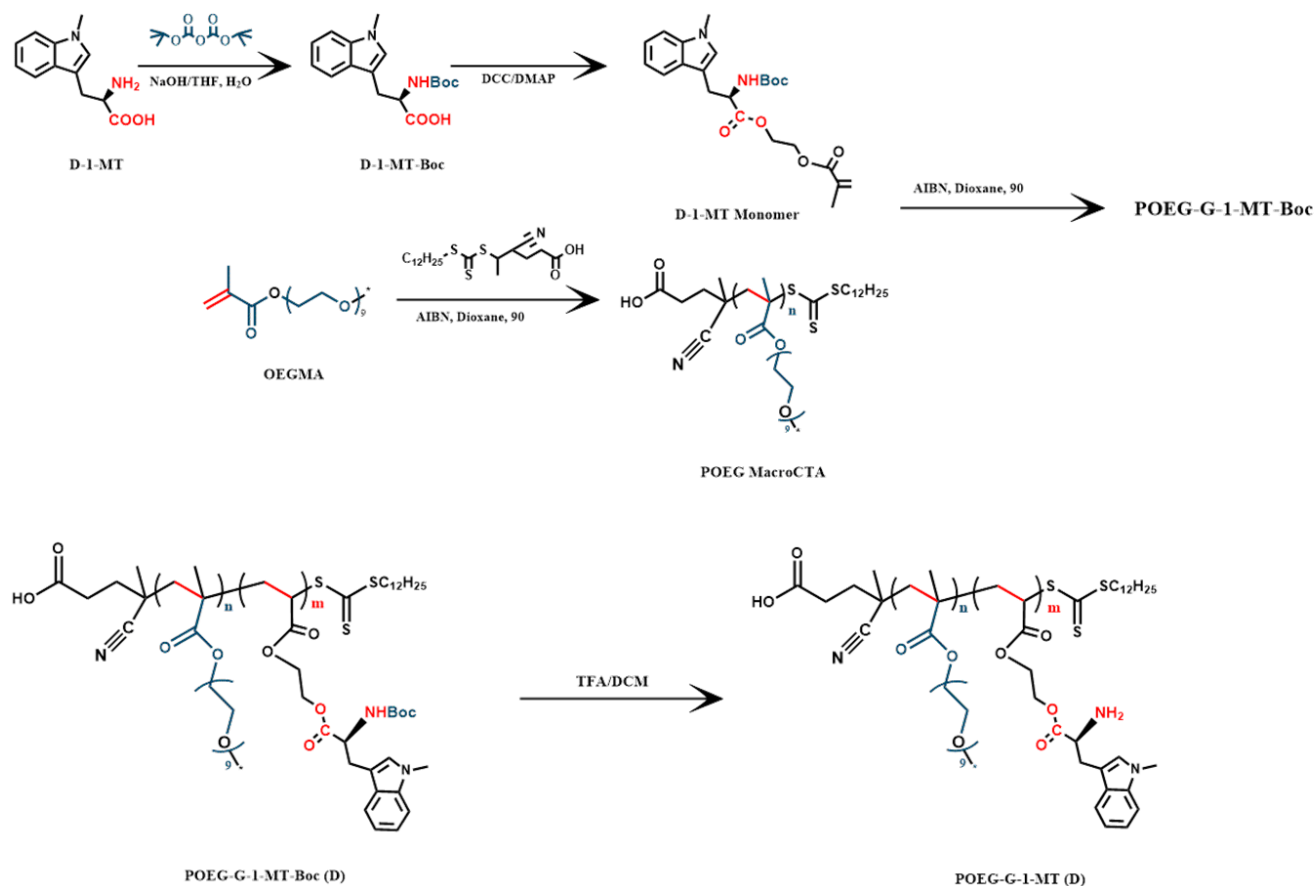## 2.2.3 Synthesis of POEG-G-1-D-MT Polymers

Figure 2. Synthesis scheme of POEG-G-1-MT polymers via RAFT polymerization

2.2.3.1 Synthesis of G-1-D-MT Monomer

1-D-MT-Boc (264mg, 0.825mmol, 1.0 eq), 2-hydroxyl methacrylate (129mg, 0.99mmol, 1.2 eq), N,N'-Dicyclohexylcarbodiimide (DCC, 205mg, 0.99mmol, 1.2 eq), and 4-Dimethylaminopyridine (DMAP, 20mg, 0.165mmol, 0.2 eq) were dissolved in 5ml DCM and the mixture was then stirred overnight at ambient temperature. The insoluble dicyclohexylurea (DCU) was filtered through cotton at first and the organic layer was collected and washed with HCl (PH=2) and saturated NaCl solution. Then, the organic solvent was removed under reduced pressure to afford a crude product. The crude was

finally purified by a column chromatograph (diethyl ether/petroleum ether, 5/5) to afford the product as a colorless oil form (264mg, 0.825mmol, 90% yield).

2.2.3.2 Synthesis of POEG-G-1-D-MT-Boc Polymers

POEG MacroCTA (170mg, 0.0192mmol, 1.0 eq), G-1-D-MT-Boc monomer (140mg, 0.325mmol, 16.9 eq), AIBN (2mg, 0.0122mmol) and 2ml anhydrous 1,4-Dioxane were added into a Schlenk tube. After three-times free-pump-thaw cycles, the deoxygenated mixture was immersed into a 90°C oil bath under nitrogen protection. The polymerization was stopped after 18h reaction, and then the reaction mixture was precipitated in petroleum ether for three times. The POEG-G-1-D-MT-Boc polymers were finally obtained after vacuum drying. Conversion of G-1-D-MT-Boc monomer was 50%.

2.2.3.3 Deprotection of POEG-G-1-D-MT-Boc Polymers

The POEG-G-1-D-MT-Boc polymers were de-protected in the mixture solution of DCM/TFA (6/5, v/v) at ambient temperature. After 1.5 hours, the reaction mixture was precipitated in diethyl ether for one time. The crude product was dissolved in the mixed solvents of DCM/Ethanol and was then precipitated by ether again. The de-protected polymers were dried in vacuum to give the product in a sticky and brown oil form.
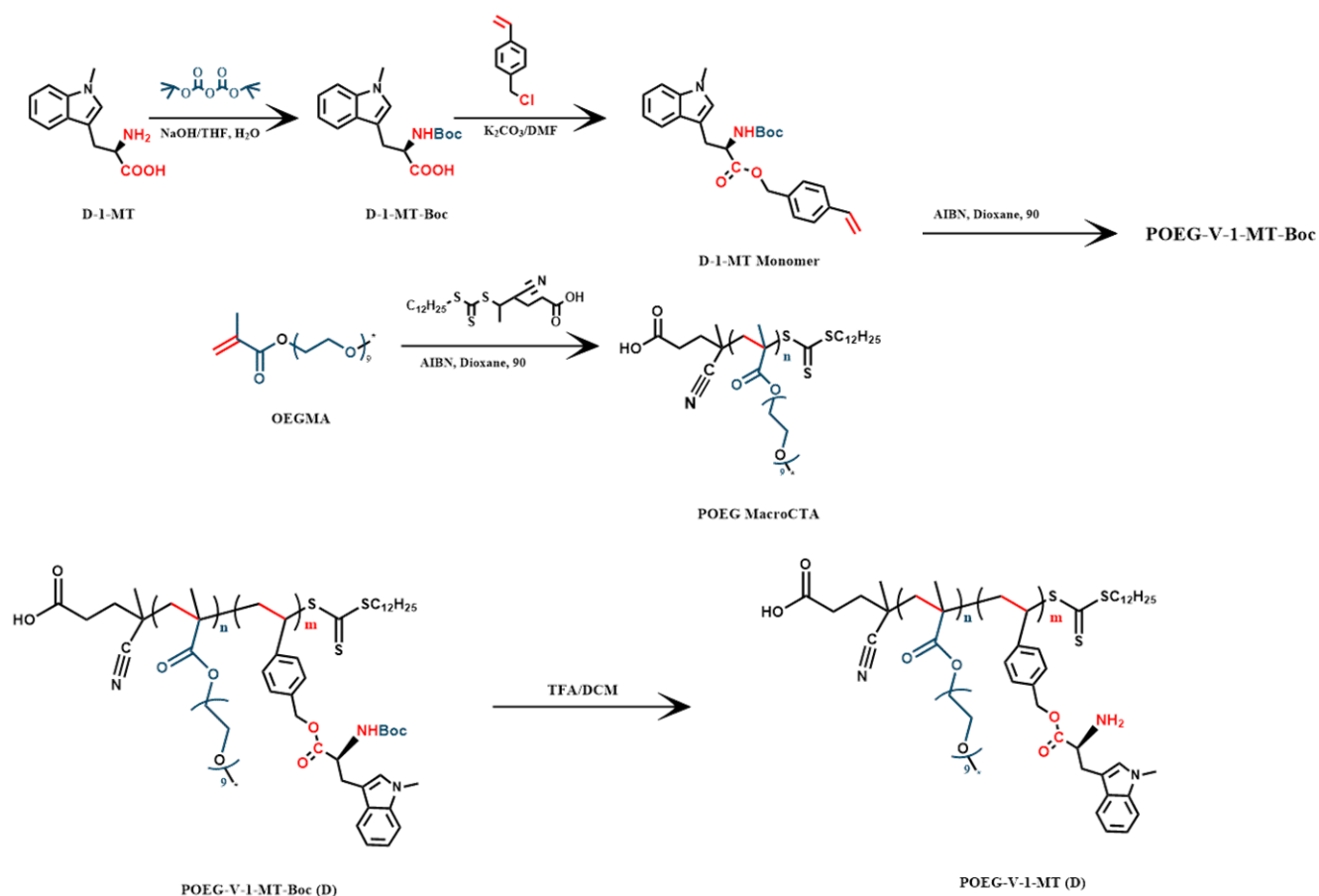
2.2.4 Synthesis of POEG-V-1-D-MT Polymers

Figure 3. Synthesis scheme of POEG-V-1-MT polymers via RAFT polymerization

2.2.4.1 Synthesis of V-1-D-MT-Boc Monomer

1-D-MT-Boc (264mg, 0.825mmol, 1.0 eq), vinylbenzyl chloride (130mg, 0.852mmol, 1.03 eq) and K_2CO_3 (571mg, 4.13 mmol, 5.0 eq) were dissolved in 5.5ml DMF and the mixture was then stirred overnight at 50°C. The cooled reaction mixture was transferred to 50ml water and the crude product was extracted by DCM. The organic phase was collected and washed by H_2O for three times to remove the remaining DMF and K_2CO_3. Then the organic phase was evaporated to give the crude product,

following being dried by sodium sulfate. The purified product was given via silica gel chromatography (diethyl ether/petroleum ether, 1/9). The V-1-D-MT-BOC monomer was finally obtained in a colorless yellow oil form.

2.2.4.2 Synthesis of POEG-V-1-D-MT-Boc Polymers

POEG MacroCTA (194mg, 0.0219mmol, 1.0 eq), G-1-D-MT-Boc monomer (161mg, 0.371mmol, 14.5 eq), AIBN (1.4mg, 0.00852mmol) and 2.3ml anhydrous 1,4-Dioxane were added into a Schlenk tube. The mixture was de-oxygenated for three times using a free-pump-thaw method. Then the tube was immersed in an oil bath at 90 ℃. After polymerization for 5 hours/18 hours, POEG-V-1-D-MT$_5$-Boc polymers and POEG-V-1-D-MT$_{10}$-Boc polymers were obtained separately. The crude product was further purified using a petroleum precipitation method for three times, and the polymers were given after vacuum drying.

2.2.4.3 Deprotection of POEG-V-1-D-MT-Boc Polymers

The Boc groups of POEG-V-1-D-MT-Boc polymers were de-protected in DCM/TFA (v/v: 6/4) at ambient temperature for 1.2 hours. Then the reaction mixture was precipitated in diethyl ether for one time. The crude product was dissolved in the mixed solvents of DCM/Ethanol and was then precipitated by ether again. The de-protected polymers were dried in vacuum to give the product in a sticky and brown oil form.

2.3 PREPEATATION OF MICELLES

2.3.1 Preparation of POEG-G-1-D-MT Based Blank Micelles

A dialysis method was used to prepare the POEG-G-1-D-MT micellar solution. Briefly, POEG-G-1-D-MT polymers (15mg) were dissolved in 400ul DMSO, followed by dialysis against 500ml distilled water for 24h. The dialysis bag is with 3500 molecular weight cut-off membrane.

The size distribution of POEG-G-1-D-MT based blank micelles was measured by dynamic light scattering (DLS) through a Malvern Zeta Nano-sizer.

2.3.2 Preparation of POEG-G-1-D-MT Based Plasmid Micelles

The various amounts of POEG-G-1-D-MT polymers (PH was adjusted into 5.5 with PBS buffer) were mixed with 1 μg (100 μL) of plasmid DNA in the labeled tubes, respectively. Then, these tubes were allowed to stand at minimum for half an hour at 37°C. The 2.7 μg/μL stock solution of plasmid DNA was diluted (PBS buffer: PH=5.5) into 1 μg/100 μL (7.4 μL was added into 2ml distilled water). The amount of POEG-G-1-D-MT polymers used to complex plasmid DNA was determined based on the designed N/P ratios (0.5, 1, 5, 10, 20, and 40) which were calculated as the number of nitrogen atoms (N, positively charged, polymers: 12630/12=1052.5) in POEG-G-1-D-MT polymers to the number of the phosphate groups (P, negatively charged, plasmid: $M_w/P(N)=330$) in plasmid DNA. After 30min incubation, the PH of POEG-G-1-D-MT and plasmid DNA complexation was adjusted to 7.4.

2.3.3 Preparation of POEG-V-1-D-MT Based Blank Micelles

A dialysis method was used to prepare the POEG-V-1-D-MT micellar solution. Briefly, POEG-V-1-D-MT polymers (10mg) were dissolved in 400ul DMSO, followed by dialysis against 500ml distilled water for 24h. The dialysis bag is with 3500 molecular weight cut-off membrane.

The size distribution of POEG-V-1-D-MT blank micelles was measured by DLS through a Malvern Zeta Nano-sizer. The morphology of POEG-V-1-D-MT blank micelles was observed by transmission electron microscopy (TEM).

2.3.4 Preparation of POEG-V-1-D-MT Based Dox-Loaded Micelles

The doxorubicin free base (DOX) was used for Dox-loaded micelle preparation. Doxorubicin hydrochloride (DOX.HCl) was reacted with 1.5M equivalents of trimethylamine (TEA) in DMSO for 24 hours (5mg DOX.HCl, 1.0 ml DMSO and 7ul TEA). The DOX solution and POEG-V-1-D-MT polymers (15mg) solution were homogenously mixed with a total amount of 400ul. Then, the mixed DMSO solutions were dialysis against 500ml distilled water for 24 hour, using a dialysis membrane with 3500 molecular weight cut-off at room temperature. POEG-V-1-D-MT micelles incorporating DOX were further purified through 220nm pore-sized filters to afford sterilized micelles.

The Dox concentrations of POEG-V-1-D-MT micelles were measured by a Water 2475 Fluorescence Plate Reader. The plate was read with an excitation wavelength of 490nm and the emission wavelength of 590nm. The size distribution of POEG-V-1-D-MT DOX loaded micelles was measured by DLS through a Malvern Zeta Nanosizer. The morphology of POEG-V-1-D-MT was observed by TEM.

2.4 GEL RETARDATION ASSAYS OF OF POEG-G-1-D-MT BASED PLASMID MICELLES

The running gel was prepared as follows: 50ml TAE buffer and 0.5g agarose were mixed to afford 1% agarose solution at 1min microwave heat. Then 4 ul ethidium bromide (EB) was added into the solutions to prepare the electrophoresis gel, followed by a PH 7.4 adjustment using acetic acid. After formation of the gel, the 1-D-MT polyplex with different N/P rations was loaded onto the gel (3ul loading buffer and 15ul sample, the control plasmid DNA is calculated as 1ug/200ul*15ul*15/18(6.25ul Plasmid DNA+8.75ul H_2O)). Then, the electrophoresis was carried out at a constant voltage of 100 V for 30min in TAE buffer. Free plasmid DNA bands were separated by electrophoresis and visualized using ultraviolet (UV) imaging system.

RESULTS

3.1 SYNTHESIS OF 1-D-MT BASED POLYMER

3.1.1 Synthesis of Boc-Protected 1-D-MT

1-D-MT-Boc ^{1}H NMR of 1-D-MT-Boc (400Hz, DMSO): 12.54 (s, 1H), 7.30-7.40 (d, 1H), 7.50-7.60 (d, 1H), 7.10-7.20 (brm, 2H), 6.85-7.10 (brm, 2H), 4.10-4.20 (brm, 1H), 3.72 (s, 3H), 3.00-3.10 (brm, 1H), 2.80-3.00 (brm, 1H), 1.45-1.20 (brm, 9H);
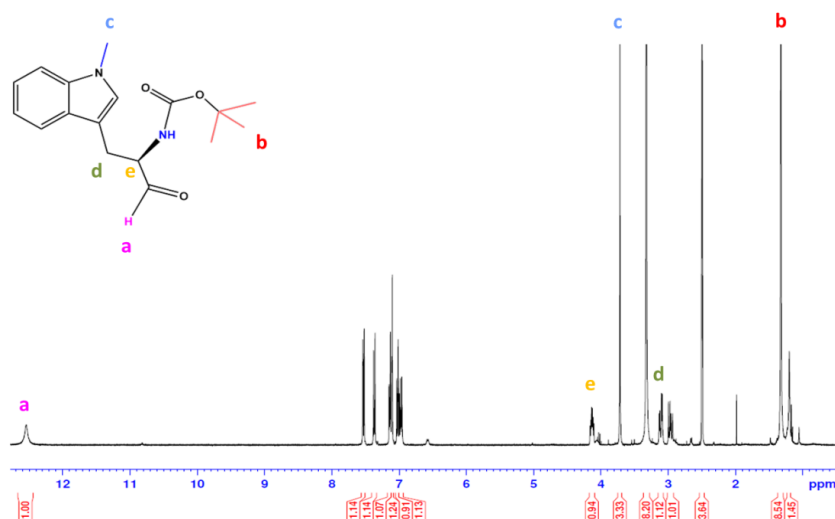

Figure 4. ^{1}H NMR spectrum of 1-D-MT-Boc in DMSO

3.1.2 Syntheis of POEG MacroCTA

POEG MacroCTA Conversion Rate ^{1}H NMR of POEG MacroCTA before purification (400Hz, CDCl$_3$): 6.15 (s, 1H), 5.60 (s, 1H), 3.37 (s, 3H), 3.65 (s, 30H);

Conversion rate of OMEGA: (1-0.14)*100%＝86%

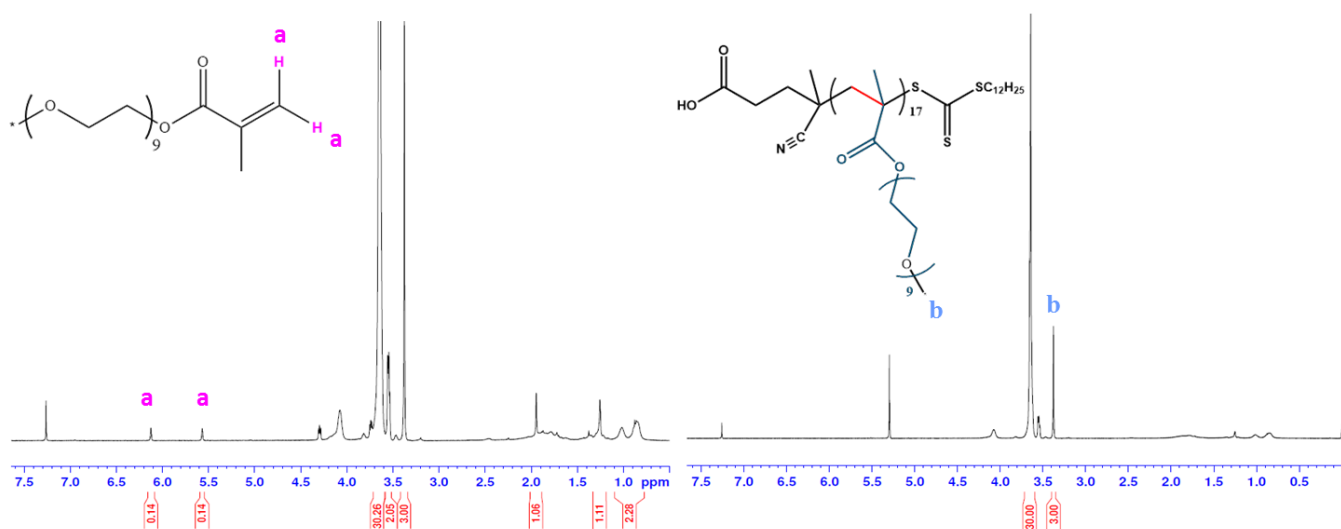(6.1 mmol/0.305mmol)* 86%＝17

Figure 5. ^{1}H NMR spectrum of POEG MacroCTA in CDCl$_3$

3.1.3 Synthesis of POEG-G-1-D-MT Polymers

3.1.3.1 Synthsis of G-1-D-MT Monomer

G-1-D-MT MONOMER ^{1}H NMR of G-1-D-MT monomer: 6.80-7.70 (brm, 6H), 6.15 (s, 1H), 5.60 (s, 1H), 4.95-5.10 (d, 1H), 4.60-4.80 (d, 1H), 4.25-4.50 (brm, 2H), 3.75 (m, 3H), 3.30 (s, 1H), 1.95 (s, 3H), 1.30-1.50 (brm, 9H);
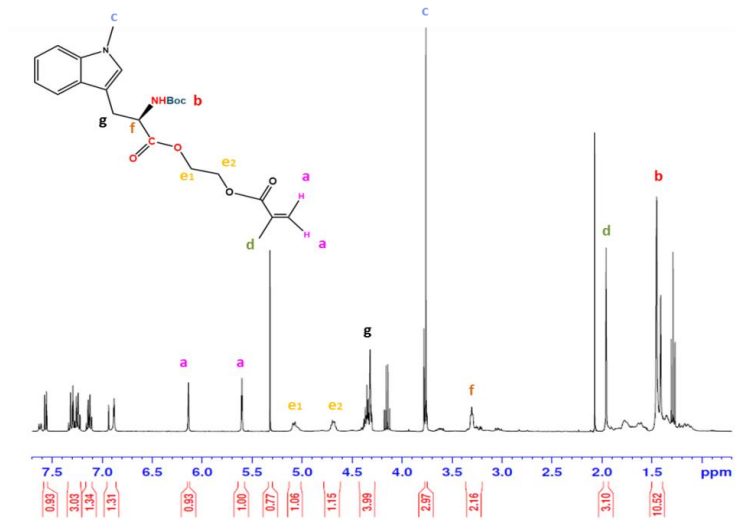
Figure 6. ^{1}H NMR spectrum of G-1-D-MT monomer in CDCl$_3$

3.1.3.2 Synthsis of POEG-G-1-D-MT-Boc Polymers

POEG-G-1-D-MT-BOC POLYMERS ^{1}H NMR of POEG-G-1-D-MT$_{10}$-Boc polymers:
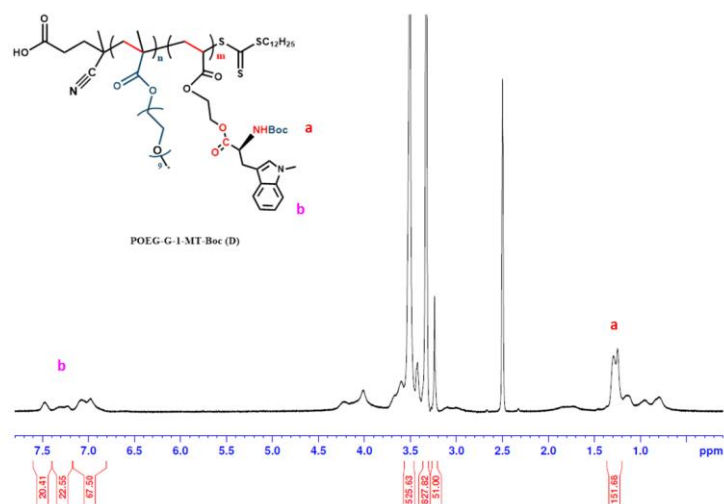

Figure 7. ^{1}H NMR spectrum of POEG-G-1-D-MT$_{10}$-Boc polymers

3.1.3.3 Synthesis of POEG-G-1-D-MT Polymers

POEG-G-1-D-MT POLYMERS ^{1}H NMR of POEG-G-1-D-MT$_{10}$ polymers:
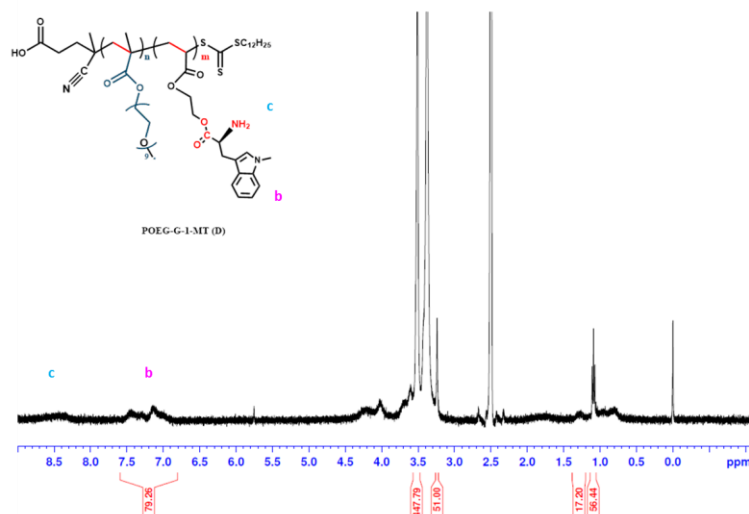

Figure 8. ^{1}H NMR spectrum of G-1-D-MT monomer in CDCl$_3$

3.1.4 Synthesis of POEG-V-1-D-MT Polymers

3.1.4.1 Synthesis of V-1-D-MT-Boc Monomer

V-1-D-MT MONOMER ^{1}H NMR of V-1-D-MT monomer: 7.00-7.80 (brm, 8H), 6.68-6.88 (brm, 1H), 6.51 (s, 1H), 5.81 (d, 1H), 5.31 (d, 1H), 5.00-5.25 (m, 2H), 4.60-4.80 (s, 1H), 3.60-3.80 (s, 3H), 3.20-3.40 (s, 2H), 1.60-1.70 (s, 1H), 1.30-1.40 (m, 9H);
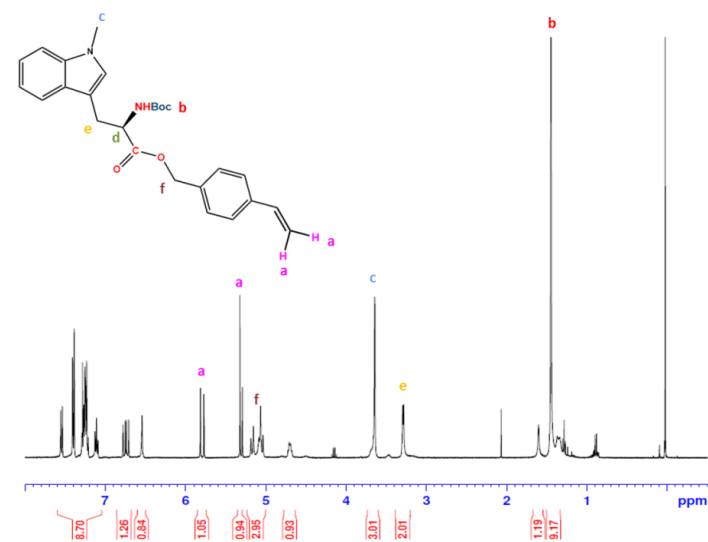
Figure 9. ^{1}H NMR spectrum of V-1-D-MT monomer in CDCl$_3$

3.1.4.2 Synthesis of POEG-V-1-D-MT4 Polymers

POEG-V-1-D-MT$_4$-Boc POLYMERS ^{1}H NMR of POEG-V-1-D-MT$_4$-Boc polymers:
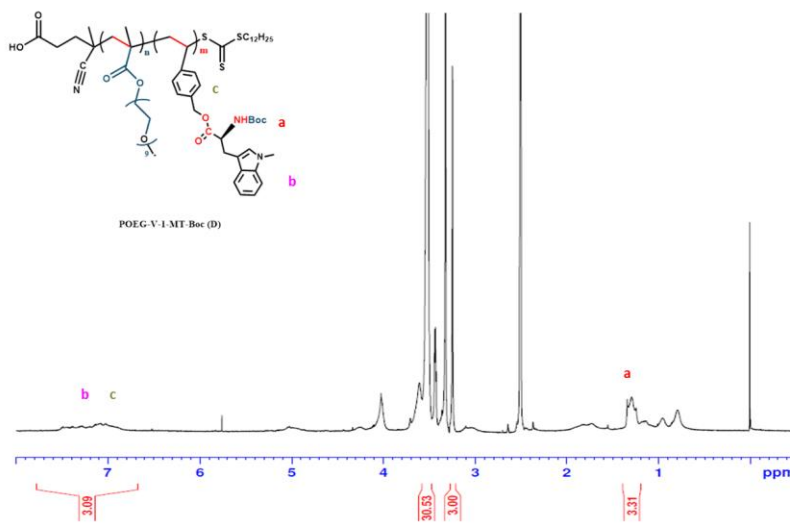
Figure 10. ^{1}H NMR spectrum of POEG-V-1-D-MT$_4$-Boc Polymers in DMSO

POEG-V-1-D-MT$_4$ POLYMERS ^{1}H NMR of POEG-V-1-D-MT$_4$ Polymers:
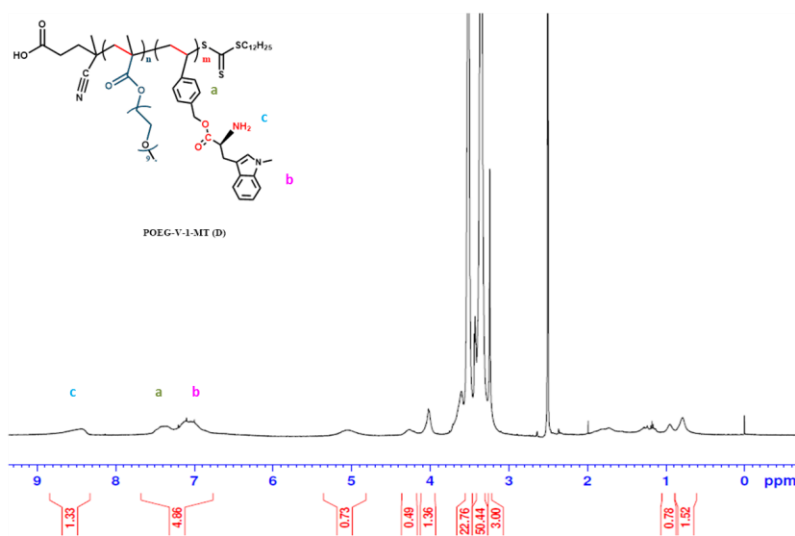
Figure 11. ^{1}H NMR spectrum of POEG-V-1-D-MT$_4$ Polymers in DMSO

3.1.4.3 Synthesis of POEG-V-1-D-MT$_{10}$ Polymers

POEG-V-1-D-MT$_{10}$-Boc POLYMERS ^{1}H NMR of POEG-V-1-D-MT$_{10}$-Boc polymers:
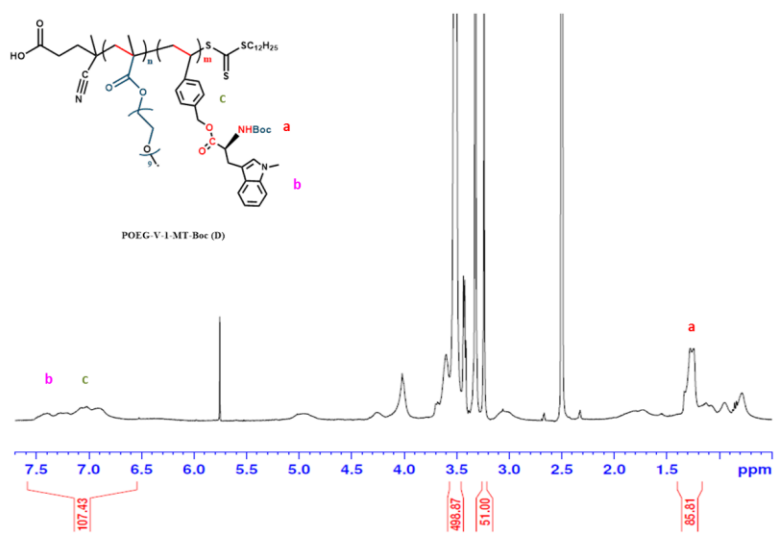
Figure 12. ^{1}H NMR spectrum of POEG-V-1-D-MT$_{10}$-Boc Polymers in DMSO

POEG-V-1-D-MT$_{10}$ POLYMERS ^{1}H NMR of POEG-V-1-D-MT$_{10}$ polymers:
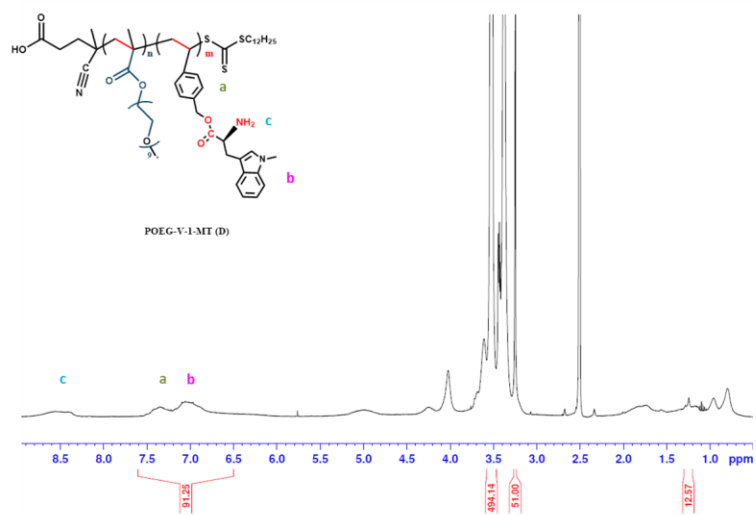
Figure 13. ^{1}H NMR spectrum of POEG-V-1-D-MT$_{10}$ Polymers in DMSO

3.2 CHARACTERIZATION OF BLANK AND DOX-LOADED MICELLES

As shown in **Figure 14**, the size of drug-free POEG-G-1MT$_{10}$ micelles demonstrated a homogenous

distribution of 92.5nm and the drug loading capacity of POEG-G-1MT$_{10}$ micelles is zero.

Table 4. Physicochemical Characterizations

Block polymer	Size(nm)	DLC(%)
POEG$_{18}$-G-1MT$_{10}$	92.5	0

Figure 14. Size distribution of drug-free POEG-G-1MT$_{10}$ micelles

As shown in **Figure 15 (A, C)**, the size of drug-free POEG-V-1MT$_4$ micelles and DOX loaded POEG-V-1MT$_4$ micelles demonstrated a homogenous distribution of 240.2nm and 90.61nm, respectively. TEM images (**Figure 15 (B, D)**) indicated spherical morphologies for both drug-free POEG-V-1MT$_4$ micelles and DOX-loaded POEG-V-1MT$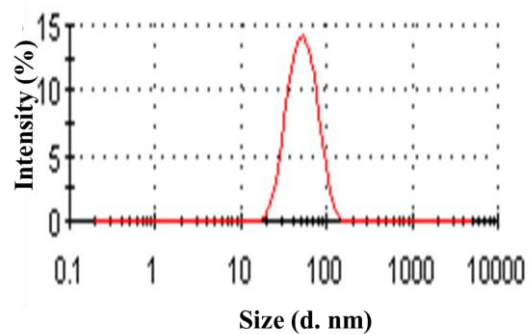_4$ micelles. As shown in **Table 5**, POEG-V-1MT$_4$ micelles showed a drug loading capacity of 28.5% and a drug loading efficiency of 52.1%.

A

POEG$_{18}$-V-1MT$_4$ (D) micelles

C

Dox/POEG$_{18}$-V-1MT$_4$ (D) mixed micelles
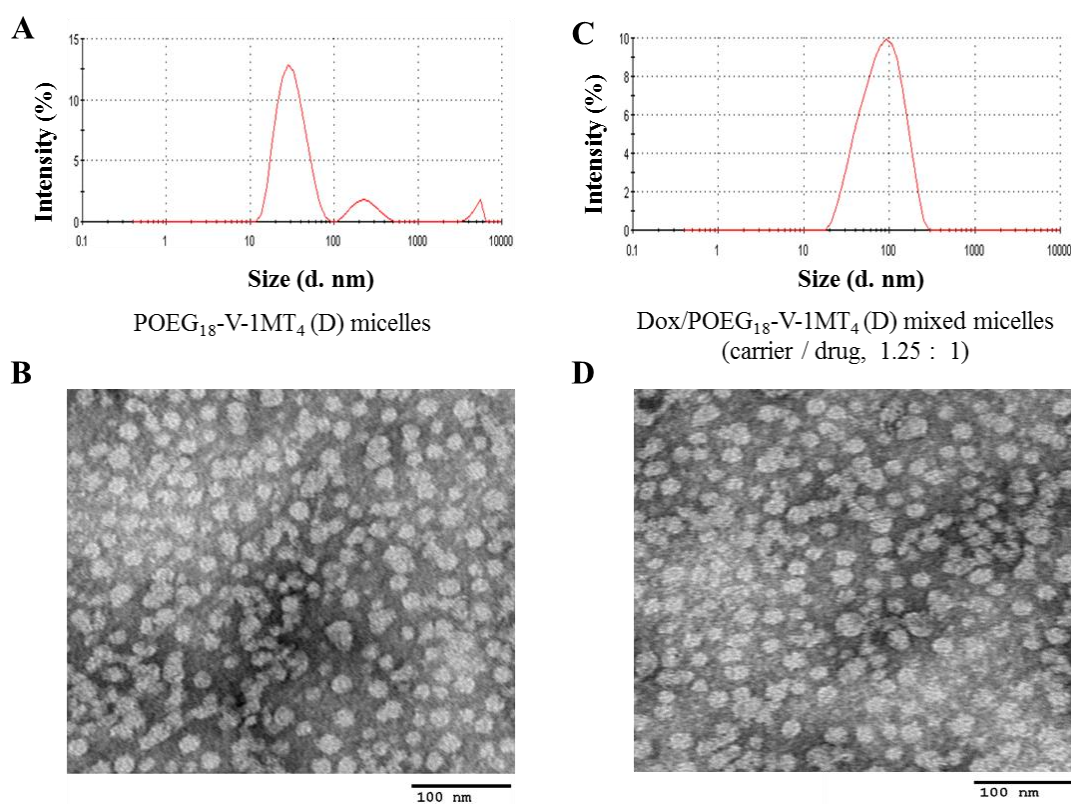(carrier / drug, 1.25 : 1)

B

D

Figure 15. Size distribution of drug-free POEG-V-1MT micelles: (A) and DOX-loaded POEG-V-1MT micelles (C). Morphology of drug-free POEG-V-1MT micelles (B) and DOX-loaded POEG-V-1MT micelles (D). Size was examined by dynamic light scattering and morphology was examined by TEM, respectively. (Scale bar, 100 nm)

Table 5. Physicochemical Characterizations

Micelles	Molar ratio	Size(nm)	PDI	Zeta Potential(mV)	DLE (%)	DLC (%)	Stability
POEG$_{18}$-V-1MT$_4$	-------	240.2	0.33	-1.23	--------	--------	14 d
POEG$_{18}$-V-1MT$_4$/ Dox	1.25 : 1	90.61	0.15	-2.34	28.5	52.1	7 d

DLE=drug loading capacity; DLC=drug loading efficiency

3.3 GEL RETARDATION ASSAY

Because plasmid DNA is negatively charged, it can run toward the positive electrode in the electrophoresis process. As complexation occurs between cationic polymers (POEG-G-1-D-MT polymers) and negatively plasmid DNA, the positive charges of POEG-G-1-D-MT polymers was neutralized by the negative charges of plasmid DNA. Therefore, the phenomenon of plasmid DNA retardation was observed. As shown in **Figure 16.,** as the N/P ratio increased from 1 to 10, the plasmid DNA band became weaker than that of the naked plasmid DNA, which indicates the partial complexation between the plasmid DNA and cationic polymers. However, the full neutralization of the plasmid DNA was not observed.
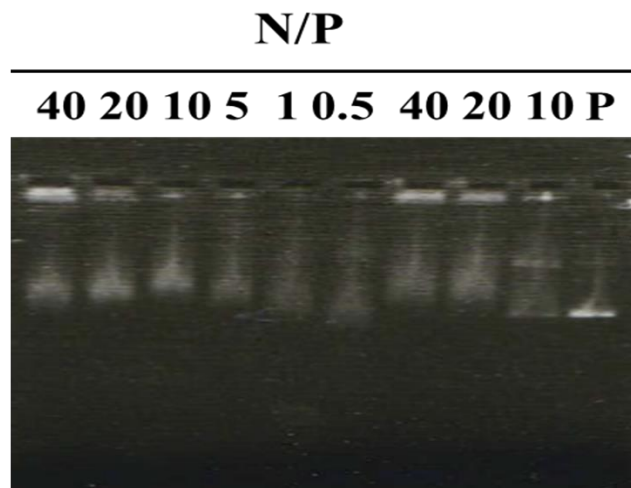
Figure 17. Gel retardation assay. POEG-G-1MT/plasmid DNA complexes at various N/P ratios were analyzed on a 1% agarose gel. The mobility of plasmid was visualized by GelRed staining. The N/P ratio of POEG-G-1MT/plasmid was 0.5, 1, 5, 10, 20 and 40. (P represents plasmid DNA)

DISCUSSION

An unblocked primary amine group remains in 1-D-MT after conjugation with PEG, whose group is positively charged and can form hydrogen bonds with water. Therefore, the inner core is not entirely hydrophobic as usual and this might have an unexpected effect on drug loading ability. Preliminary data have shown that a 1-D-MT polymer with a linear ethylene glycol vinyl ether linker can only load limited amounts of PTX and DOX. This result is consistent with our hypothesis. Furthermore, the poor loading efficiency might be due to the hydrophobicity of the indole ring as well as the charge effects of amine group. Next, the introduction of a vinylbenzyl chloride linker was found to lead to an improvement in drug loading capacity. However, there is no linear correlation between the drug loading capacity and the number of repeated 1-D-MT units and the optimal repeated units are between four and nine. This result further verifies the importance of the amine group and indole ring within the structure of 1-D-MT. More studies on the biophysical and biological properties of the new carrier are currently underway.

Generally, most of the reported polymeric prodrug micelles are constructed using a post-modification method, and the modified drug was covalently attached to the hydrophilic polymer backbone. The major disadvantage of this strategy is the complicated synthesis steps. In addition, some reactive groups, owing to the steric hindrance, might still remain in the polymer backbone following incomplete conjugation, which might lead to the destruction of the micellar structure and to undesirable side effects through interacting with potential bioactive molecules *in vivo*. In contrast, polymerization of those drug-based monomers represents a better approach to obtain well-defined amphiphilic polymeric prodrugs. By using reversible addition fragmentation transfer (RAFT) polymerization method, the batch to batch difference of the synthesized polymeric micelles can be well controlled[28]. In this work, the hydrophilic monomers and two 1-D-MT based hydrophobic monomers are prepared first, followed by

RAFT polymerization to give well-defined di-block co-polymers with fewer steps. The properties of such polymers can be adjusted with different hydrophilic POEG block/hydrophobic 1-D-MT block molar ratios and the type of linker.

In summary, our studies have shed some insights into the structure-activity relationship of 1-D-MT polymer. One such polymer was obtained that was effective in loading of both DOX and PTX in preliminary studies. More studies on the potential of this carrier for combination therapy with chemotherapeutic agents are ongoing.

BIBLIOGRAPHY

1   Senkus, E. *et al.* Primary breast cancer: ESMO Clinical Practice Guidelines for diagnosis, treatment and follow-up. *Annals of oncology : official journal of the European Society for Medical Oncology* **26 Suppl 5**, v8-30, doi:10.1093/annonc/mdv298 (2015).

2   Kipp, J. The role of solid nanoparticle technology in the parenteral delivery of poorly water-soluble drugs. *International journal of pharmaceutics* **284**, 109-122 (2004).

3   Narvekar, M., Xue, H. Y., Eoh, J. Y. & Wong, H. L. Nanocarrier for poorly water-soluble anticancer drugs—barriers of translation and solutions. *AAPS PharmSciTech* **15**, 822-833 (2014).

4   Atkins, J. H. & Gershell, L. J. Selective anticancer drugs. *Nature reviews. Drug discovery* **1**, 491 (2002).

5   Wong, H. L., Bendayan, R., Rauth, A. M., Li, Y. & Wu, X. Y. Chemotherapy with anticancer drugs encapsulated in solid lipid nanoparticles. *Advanced drug delivery reviews* **59**, 491-504 (2007).

6   Davis, S. T. *et al.* Prevention of chemotherapy-induced alopecia in rats by CDK inhibitors. *Science* **291**, 134-137 (2001).

7   Wang, A. Z., Langer, R. & Farokhzad, O. C. Nanoparticle delivery of cancer drugs. *Annual review of medicine* **63**, 185-198 (2012).

8   Shi, J., Kantoff, P. W., Wooster, R. & Farokhzad, O. C. Cancer nanomedicine: progress, challenges and opportunities. *Nature Reviews Cancer* (2016).

9   Bertrand, N., Wu, J., Xu, X., Kamaly, N. & Farokhzad, O. C. Cancer nanotechnology: the impact of passive and active targeting in the era of modern cancer biology. *Advanced drug delivery reviews* **66**, 2-25, doi:10.1016/j.addr.2013.11.009 (2014).

10   Clark, A. J. *et al.* CRLX101 nanoparticles localize in human tumors and not in adjacent, nonneoplastic tissue after intravenous dosing. *Proceedings of the National Academy of Sciences of the United States of America* **113**, 3850-3854, doi:10.1073/pnas.1603018113 (2016).

11   Lee, H. *et al.* 64Cu-MM-302 Positron Emission Tomography Quantifies Variability of Enhanced Permeability and Retention of Nanoparticles in Relation to Treatment Response in Patients with Metastatic Breast Cancer. *Clinical cancer research : an official journal of the American Association for Cancer Research*, doi:10.1158/1078-0432.ccr-16-3193 (2017).

12   Xiong, X.-B., Falamarzian, A., Garg, S. M. & Lavasanifar, A. Engineering of amphiphilic block copolymers for polymeric micellar drug and gene delivery. *Journal of controlled release* **155**, 248-261 (2011).

13   Croy, S. & Kwon, G. Polymeric micelles for drug delivery. *Current pharmaceutical design* **12**, 4669-4684 (2006).

14   Lake, R. A. & Robinson, B. W. Opinion: Immunotherapy and chemotherapy--a practical partnership. *Nature reviews. Cancer* **5**, 397 (2005).

15   Zitvogel, L., Apetoh, L., Ghiringhelli, F. & Kroemer, G. Immunological aspects of cancer chemotherapy. *Nature reviews. Immunology* **8**, 59 (2008).

16   Kroemer, G., Galluzzi, L., Kepp, O. & Zitvogel, L. Immunogenic cell death in cancer therapy. *Annual review of immunology* **31**, 51-72 (2013).

17 Barbee, M. S., Ogunniyi, A., Horvat, T. Z. & Dang, T.-O. Current status and future directions of the immune checkpoint inhibitors ipilimumab, pembrolizumab, and nivolumab in oncology. *Annals of Pharmacotherapy* **49**, 907-937 (2015).

18 Munn, D. H. & Bronte, V. Immune suppressive mechanisms in the tumor microenvironment. *Current opinion in immunology* **39**, 1-6 (2016).

19 Munn, D. H. & Mellor, A. L. IDO in the tumor microenvironment: inflammation, counter-regulation, and tolerance. *Trends in immunology* **37**, 193-207 (2016).

20 Austin, C. J. & Rendina, L. M. Targeting key dioxygenases in tryptophan–kynurenine metabolism for immunomodulation and cancer chemotherapy. *Drug discovery today* **20**, 609-617 (2015).

21 Vacchelli, E. *et al.* Trial watch: IDO inhibitors in cancer therapy. *Oncoimmunology* **3**, e957994 (2014).

22 Opitz, C. A. *et al.* The indoleamine-2, 3-dioxygenase (IDO) inhibitor 1-methyl-D-tryptophan upregulates IDO1 in human cancer cells. *PloS one* **6**, e19823 (2011).

23 Soliman, H. H. *et al.* A first in man phase I trial of the oral immunomodulator, indoximod, combined with docetaxel in patients with metastatic solid tumors. *Oncotarget* **5**, 8136 (2014).

24 Mautino, M. *et al.*   (Google Patents, 2016).

25 Lutz, J. F. Polymerization of oligo (ethylene glycol)(meth) acrylates: toward new generations of smart biocompatible materials. *Journal of Polymer Science Part A: Polymer Chemistry* **46**, 3459-3470 (2008).

26 Chiefari, J. *et al.* Living free-radical polymerization by reversible addition– fragmentation chain transfer: the RAFT process. *Macromolecules* **31**, 5559-5562 (1998).

27 Huang, Y., Liu, Y., Liu, Y., Song, H. & Wang, Q. C ring may be dispensable for β-carboline: design, synthesis, and bioactivities evaluation of tryptophan analog derivatives based on the biosynthesis of β-carboline alkaloids. *Bioorganic & medicinal chemistry* **24**, 462-473 (2016).

28 Chong, Y., Le, T. P., Moad, G., Rizzardo, E. & Thang, S. H. A more versatile route to block copolymers and other polymers of complex architecture by living radical polymerization: the RAFT process. *Macromolecules* **32**, 2071-2074 (1999).